Asian Journal of Chemistry; Vol. 25, No. 4 (2013), 1937-1941

ASIAN JOURNAL OF CHEMISTRY

http://dx.doi.org/10.14233/ajchem.2013.13245

Thermal Decomposition Investigation of $Zn_4O(NH_2\text{-}BDC)_3$ (IRMOF-3) and NH_2-BDC by *in situ* DRIFTS

FANG ZHANG, CHAO CHEN*, LI XU and NING ZHANG*

Department of Chemistry, Nanchang University, Nanchang 330031, P.R. China

*Corresponding author: Fax: +86 791 3969514; Tel: +86 791 3969514; E-mail: chaochen@ncu.edu.cn; nzhang.ncu@163.com

(*Received*: 14 December 2011; *Accepted*: 8 October 2012) AJC-12254

The thermal decomposition of a porous amino metal-organic framework, $Zn_4O(NH_2\text{-}BDC)_3$ (IRMOF-3), has been investigated comparatively by *in situ* diffuse reflectance infrared Fourier transform spectroscopy (DRIFTS) and TG techniques. FT-IR, PXRD, N_2 adsorption-desorption and elemental analyses were applied to confirm the compositions of products. As revealed by these analyses, the ligand in IRMOF-3 exhibits different thermal decomposition behaviour than does the free ligand. Possible decomposition pathways are proposed. In addition, mesoporous carbon possessing a high BET surface area was obtained from thermal decomposition of IRMOF-3 at 800 ºC.

Key Words: *In situ* DRIFTS, Decomposition, IRMOF-3, Mesoporous carbon.

INTRODUCTION

Metal-organic frameworks (MOFs) have attracted extensive attention in recent years owing to their intriguing structural motifs and potential applications[1-4]. One major disadvantage of MOFs is their limited thermal stabilities, which prevents them from competing with inorganic zeolites in some practical applications. To use them much better at relative high temperature or improve their thermal stabilities, it is essential to understand how such materials decompose. However, the decomposition detail and mechanism study of MOFs are rare because *in situ* study is a challenge. Recently, the TG coupled with mass (TG-MS) or IR (TG-IR) techniques have been introduced to study the decomposition of several MOFs[5-10], but they only provide the *in situ* information of gas products. The detailed decomposition processes of MOFs, such as reactions occurring, the solid intermediates, are still hard to be directly probed by aforementioned techniques. In this study, it is noticed that *in situ* diffuse reflectance infrared Fourier transform spectroscopy (DRIFTS), extensively employed to understand the mechanism of catalytic reaction, can track the decomposition process and offer the information *in situ* by monitoring the IR absorption of reaction products. It might facilitate to understand the decomposition mechanism of MOFs.

In this work, IRMOF-3, a well-known amino MOFs with a cubic topology prepared from $Zn(NO_3)_2{\cdot}4H_2O$ and 2-amino-1,4-benzene dicarboxylic acid (NH_2-BDC), was selected as representative MOF for thermal decomposition study since it possesses following characteristics: (1) Many applications of IRMOF-3 were reported on gas adsorption, catalyst, especially on functionalization of amino group by postsynthetic modification (PSM) because of its ability to be functionalized facilely[11-14]; (2) its amino, side groups of organic linkers can not only change the flexible character of framework and thus its thermal stability, but also may show different decomposition behaviour compared to corresponding free organic linkers, which will be in favor of the further study on decomposition mechanism of complicated MOFs.

Herein, the thermal decomposition processes of IRMOF-3 and the corresponding free ligand (NH_2-BDC) were investigated comparatively by combining *in situ* DRIFTS as well as TG. And the thermal decomposition products were characterized by the IR, PXRD, N_2 adsorption-desorption and elemental analyses. This work provides important decomposition information of $-NH_2$ group and carboxyl group of IRMOF-3. Furthermore, mesoporous carbon was obtained from thermal decomposition of IRMOF-3 at 800 ºC.

EXPERIMENTAL

Synthesis of IRMOF-3: IRMOF-3 was synthesized using previously reported methods and characterized by IR spectrum (Fig. 1). The phase purity and structure of as-synthesized sample was confirmed by PXRD[15]. As shown in Fig. 2, the PXRD pattern of as-synthesized sample is uniform to that of reported IRMOF-3, indicating successful synthesis of IRMOF-3 and the phase purity of the bulk sample.

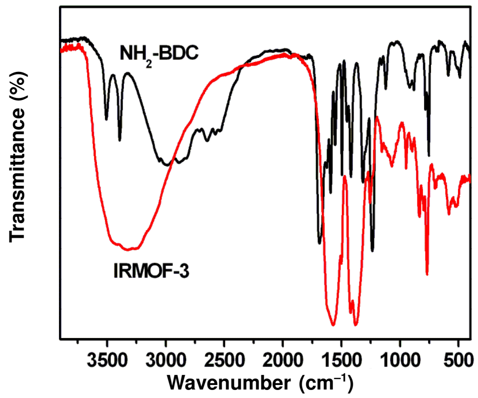

Fig. 1. FT-IR spectra for IRMOF-3 and NH_2-BDC. FT-IR spectra were recorded as KBr discs on a Nicolet-5700 spectrophotometer in the 4000-400 cm^{-1} regions

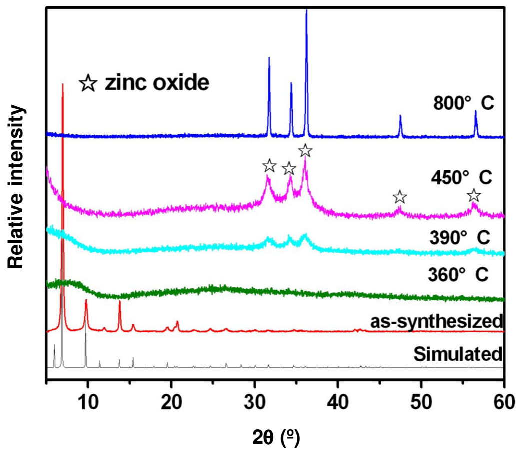

Fig. 2. PXRD patterns of IRMOF-3 calcined at different temperatures

Characterization: The contents of C, H and N were obtained by means of elemental analysis using a vario EL CUBE apparatus. Powder X-ray diffraction (PXRD) data was collected on a Rigaku D/MAX-IIIA diffractometer with CuK_α radiation (λ = 1.5418 Å). Thermogravimetric measurements were carried out from room temperature to 800 ºC on a TA SDT-Q600 thermogravimetric analyzer with a heating rate of 10 ºC min^{-1} in nitrogen. Nitrogen adsorption and desorption isotherms were performed at -196 ºC in a Micromeritics ASAP 2020 volumetric adsorption system. The samples were outgassed for 5 h at 350 ºC before the measurements. The pore-size distribution was calculated using the Barrett-Joyner-Halenda (BJH) model. FT-IR spectra of samples as KBr discs were recorded pellets on a Nicolet-5700 spectrophotometer over the range 4000-400 cm^{-1}.

In situ DRIFTS of samples were carried out with a Nicolet-5700 apparatus equipped with an MCT detector and cooled by liquid nitrogen. The samples were placed into the infrared cell, which equipped with temperature controlled parts that allowed samples to be heated to 600 ºC and ZnSe window. The spectra were recorded at 4 cm^{-1} resolution and 64 scans were accumulated for each spectrum in the spectral range of 4000-650 cm^{-1} under nitrogen atmosphere (30 mL min^{-1}). IRMOF-3 and NH_2-BDC were pretreated with nitrogen (30 mL min^{-1}) at 150 ºC for 2 h.

RESULTS AND DISCUSSION

Thermal stability: The thermal stability of IRMOF-3 was studied by the TG and PXRD analyses (Fig. 3a). The TG curve shows that the weight loss between 30 and 360 ºC can be assigned to solvent molecules. The PXRD pattern of the solvent free phase reveals that the crystalline of the IRMOF-3 can not be maintained after removing the solvent molecules. Further rising the temperature, IRMOF-3 starts to decompose and produces ZnO. For comparison, the TG curve of NH_2-BDC was also recorded. As shown in Fig. 3b, a sharp weight loss is observed when heated to 300 ºC, which is lower than the decomposition temperature of IRMOF-3.

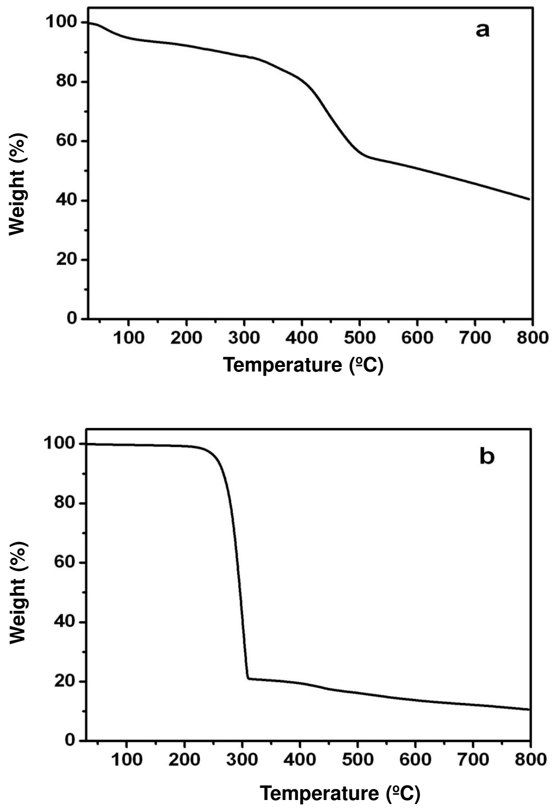

Fig. 3. TG curves of IRMOF-3 (a) and NH_2-BDC (b)

***In situ* DRIFTS analysis:** *In situ* DRIFTS was used to monitor the thermal decomposition process of the IRMOF-3. It can track the reaction intermediates and products under high temperatures or high pressures, thus provides the direct evidence for the reaction mechanism[16,17]. The DRIFT spectra of IRMOF-3 and NH_2-BDC at different temperatures were depicted in Fig. 4a-c, respectively. As illustrated in Fig. 4a, the doublet at 3410 and 3520 cm^{-1} corresponds to the symmetric and asymmetric stretching of the amine moieties. Compared to the bands of $-NH_2$ group in NH_2-BDC (at 3390 and 3500 cm^{-1}, Fig. 4c), the bands are broader and shift to higher wavenumber, which is possible due to the hydrogen-bonding interaction in IRMOF-3. The adsorption at 3056 cm^{-1} is related to the C-H stretching of ligand. The bands at 2351 and 671 cm^{-1} are, respectively ascribed to the asymmetric stretching and bending vibrations of CO_2. And the bands at 2223 cm^{-1} is assigned to asymmetric stretching of CO molecules, which

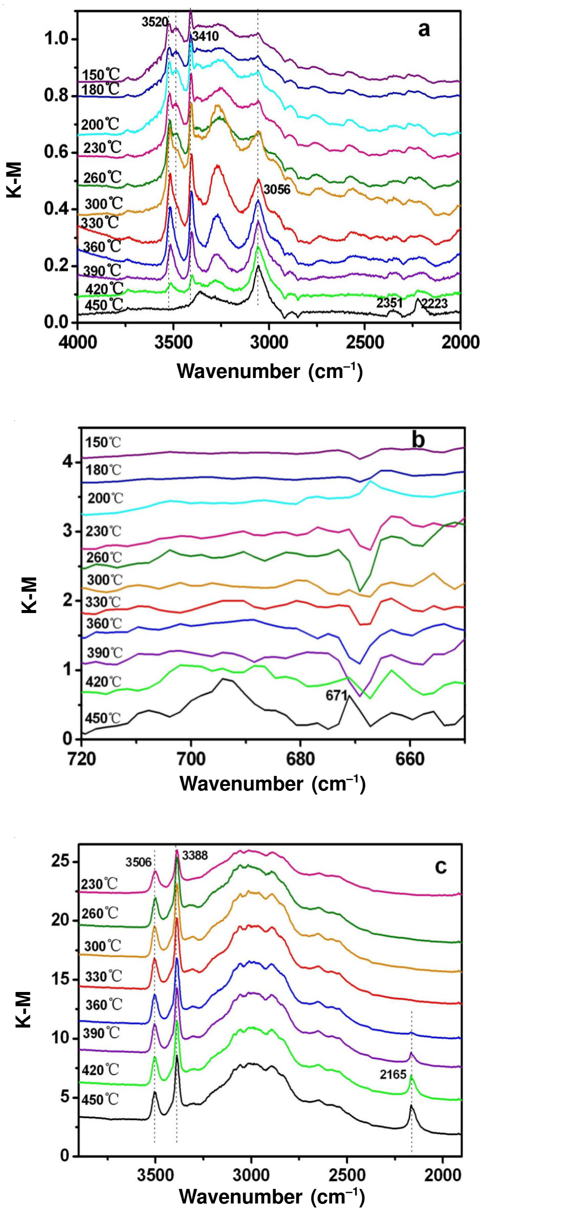

Fig. 4. DRIFT spectra of IRMOF-3 (a and b) and NH_2-BDC (c) at various temperatures. Each spectrum has been taken 10 min after the desired temperature reached

is higher than that in NH_2-BDC (2165 cm^{-1}). It might be due to the fact that CO attracted electron from ZnO *via* crystal decomposed, which is similar to the Lavalley's observation[18].

As revealed in Fig. 4c, the observation of the band at 2165 cm^{-1} above 360 ºC suggests the decomposition of carboxyl groups. While the intensities of band at 3390 and 3500 cm^{-1} virtually unaltered over the entire temperature range, which indicates that the $-NH_2$ group of NH_2-BDC is stable at 450 ºC. It is noteworthy the different thermal stability of NH_2-BDC is observed between the TG and *in situ* DRIFTS techniques. It probably comes from partial vaporization of NH_2-BDC that can not be carried away by N_2 in the infrared cell.

Fig. 4a demonstrates that the shoulder band at 3485 cm^{-1} is gradually disappeared and the stretching band of N-H is red-shifted and becomes clearer with the increase of temperature. The reason is attributed to the loss of solvent molecules. Subsequent to higher temperature treatment, the intensity of the bands at 3410 and 3520 cm^{-1} decreases at 390 ºC and disappears at 450 ºC, indicating the decomposition of the $-NH_2$ group. It can be verified by elemental analysis (%) calculated: C 35.4, N 5.2; 450 ºC: C 16.6, N 2.6 (Table-1). Simultaneously, the observation of the bands at 2223, 2351 and 671 cm^{-1} at 420 and 450 ºC suggests the formation of CO_2 and CO which indicates the decomposition of carboxyl group. These are in accordance with the TG analysis. It should be pointed out that the band at 3056 cm^{-1} is not shifted in the examined temperature range, which indicates that the aromatic ring is not destructed.

The comparison of the two decomposition processes reveals that the $-NH_2$ group of IRMOF-3 is less thermally stable than that of NH_2-BDC. The discrepancy can be explained as follows. As shown in Fig. 5a, IRMOF-3 features the Zn_4O clusters linked by NH_2-BDC[19]. Intramolecular hydrogen bonds are possible formed between amine and carboxyl groups (Fig. 6). The intramolecular hydrogen bond and Zn ion may accelerate the cleavage of the $-NH_2$ group[20]. Zn_4O take an effect on the losing of $-COO^-$ and $-NH_2$ by electron transfer *via* $O^{2-}Zn^{2+} \rightarrow O^-Zn^+$ ligand-to-metal charge transfer[21]. Furthermore, the two decomposition processes demonstrate that both CO_2 and CO are obtained by breaking the carboxylic groups of IRMOF-3 while only CO is formed from NH_2-BDC. This is because that the cleavage of carboxylato groups in IRMOF-3 tends to form CO_2. These results about the thermal behaviours of IRMOF-3 and free ligand, especially for the $-NH_2$ group, are helpful for the utilization of IRMOF-3.

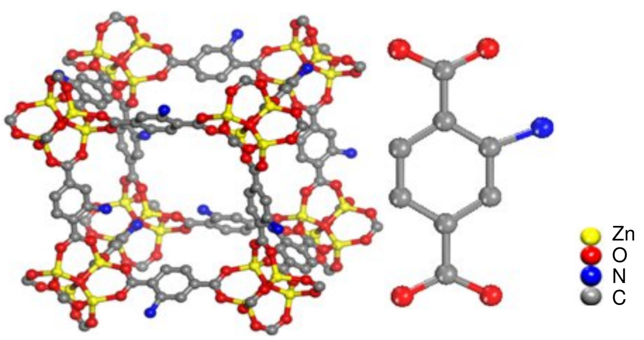

Fig. 5. View of the framework connectivity of IRMOF-3 (a) and NH_2-BDC (b). All the hydrogen atoms are omitted for clarity

TABLE-1
ELEMENTAL ANALYSIS OF IRMOF-3 AND NH_2-BDC

	IRMOF–3						NH_2–BDC					
T (ºC)	25	360	390	420	450	800	25	360	390	420	450	800
C (%)	35.4	32.0	28.2	16.6	12.6	12.8	53.0	63.5	66.0	68.5	68.0	72.9
H (%)	1.8	2.7	2.5	1.5	1.5	4.3	3.9	3.8	6.0	4.0	6.7	6.4
N (%)	5.2	4.9	4.3	2.6	2.6	1.9	7.7	10.3	10.9	11.8	11.8	7.5
C/N	6.8	6.5	5.8	6.2	4.9	6.7	6.9	6.2	6.1	5.8	5.8	9.7

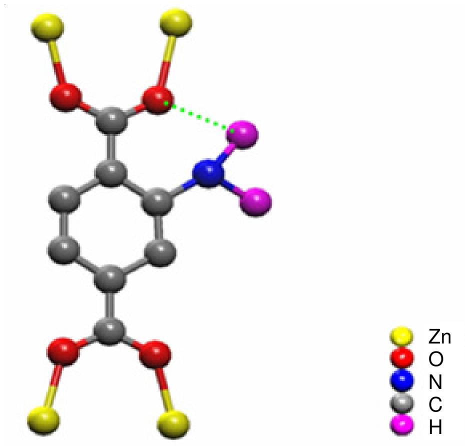

Fig. 6. Optimized structural geometry of IRMOF-3. An intramolecular hydrogen bond reinforces the co-planarity of the benzene ring and the zinc-oxo carboxylato ring, increasing the electron delocalization[1]

Mesoporous carbon obtained from thermal decomposition of IRMOF-3 at 800 ºC: Mesoporous carbon has attracted much interest owing to potential technological applications[22]. Several MOFs have been utilized as good precursors to synthesize these interesting porous carbon materials[23]. Herein, IRMOF-3 was calcined at 800 ºC in N_2 and the resulting black powder was characterized by elemental analysis, PXRD and N_2 adsorption-desorption. Elemental analysis reveals that the black powder consists of C, N and H (C 12.8, N 1.9, H 4.3), where the N is probably from the decomposition of -NH_2 group or nitrogen atmosphere and the H comes from the H_2O when it was exposed to air. Prior to nitrogen adsorption-desorption measurement, the black powder was pretreated by hydrochloric acid to remove ZnO (Fig. 7). The residue exhibits the IV isotherms with hysteresis loops, indicating the presence of mesoporous structure (Fig. 8). It is also evidenced by the diffraction peak at small-angle of PXRD pattern (Fig. 7). Moreover, the pore-size distribution curve shows its bimodal structure and the BET surface area can attain 1435 m^2 g^{-1}.

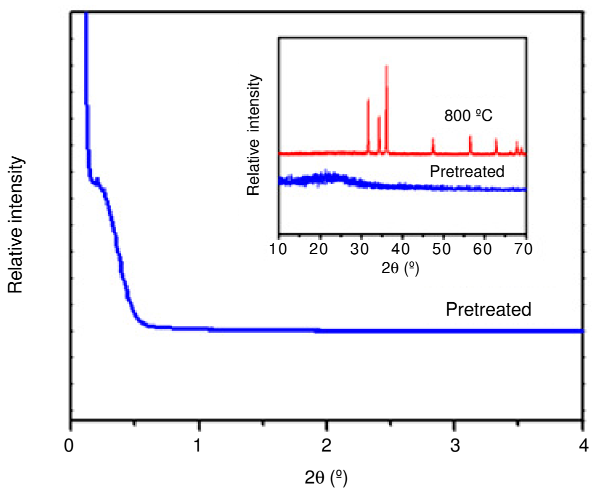

Fig. 7. PXRD patterns of IRMOF-3 calcined at 800 ºC and then washed by hydrochloric acid and water. Diffraction peaks of ZnO disappeared, indicating that ZnO has removed. And there are peaks in the PXRD patterns at a small-angle, which indicated that carbon calcination at 800 ºC is mesoporous structure

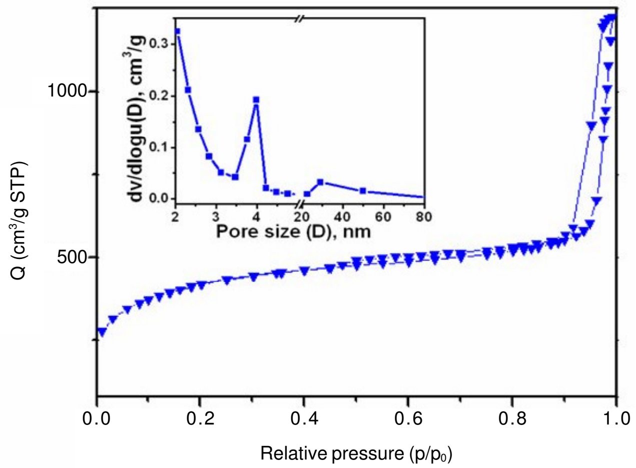

Fig. 8. Nitrogen adsorption-desorption isotherms and pore size distributions

Possible thermal decomposition mechanism: From the above results and discussion, the IRMOF-3 and NH_2-BDC exhibit different decomposition processes. As shown in **Scheme-I**, for IRMOF-3, there are four types of bond cleavages: (I) the cleavage of the C-N; (II) the Zn-O breaking between the Zn_4O cluster and carboxylic group; (III) the C-C breaking between carboxylic group and aromatic ring; (IV) the cleavage of C-O. The type I cleavage produces the nitrogen and nitride with losing the hydrogen atoms and accepting oxygen atoms, respectively. The II, III and IV cleavages gave the CO_2, CO and ZnO. Furthermore, the aromatic ring intermediates can be formed *via* I and II cleavages. The intermediates can connect to each other to form carbon species with releasing hydrogen atoms and it also might be able to accept hydrogen atoms to form benzene molecules. For NH_2-BDC, two types of cleavages are observed at relative lower temperature (≤ 450 ºC). One is the C-C breaking between the carboxylic group and aromatic ring. The other is the C-O breaking between carbonyl and hydroxyl groups. The two cleavages result in the formation of CO. When elevating the temperature, the cleavage of C-N may occur and form the nitrogen and nitride like the IRMOF-3. At the same time, the aromatic intermediates can also form carbon species confirmed by the elemental analysis (Table-1).

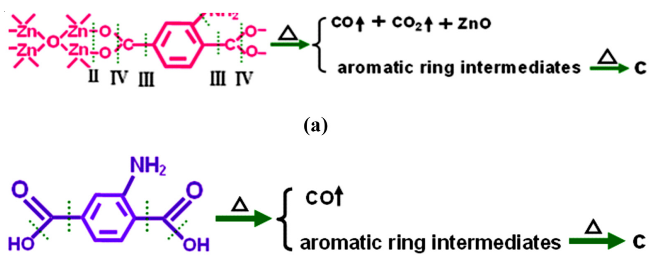

Scheme-I: Possible thermal decomposition mechanism of IRMOF-3 (a) and NH_2-BDC (b)

Conclusion

The thermal decomposition behaviours of IRMOF-3 and NH_2-BDC were firstly systematically investigated by *in situ* DRIFTS. The ligand of IRMOF-3 exhibits different thermal decomposition behaviour as compared with free ligand

NH_2-BDC. And the intramolecular hydrogen bond and structural features of framework are responsible for above discrepancy. The study of thermal decomposition is helpful for the exploitation of IRMOF-3 on applications.

ACKNOWLEDGEMENTS

This work was supported by the National Natural Science Foundations of China (No. 20701018 and 21062013), the Foundation of Educational Department of Jiangxi Province (GJJ08024) and a fellowship to Dr. C. Chen from the China Scholarship Council.

REFERENCES

1. R. Vaidhyanathan, S.S. Iremonger, G.K.H. Shimizu, P.G. Boyd, S. Alavi and T.K. Woo, *Science*, **330**, 650 (2010).
2. Z.X. Zhao, Z. Li and Y.S. Lin, *Ind. Eng. Chem. Res*., **48**, 10015 (2009).
3. A. Dhakshinamoorthy, M. Alvaro and H.A. Garcia, *Catal. Sci. Technol*., **1**, 856 (2011).
4. Z.J. Liang, M. Marshall and A.L. Chaffee, *Energy Fuels*, **23**, 2785 (2009).
5. M. Mehring, M. Elsener and O. Kroecher, *J. Therm. Anal. Calorim*., **105**, 545 (2011).
6. B.A. Howell, Y.J. Cho and Z.R. Feng, *J. Therm. Anal. Calorim*., **106**, 63 (2011).
7. B.A. Howell and Y.J. Cho, *J. Therm. Anal. Calorim*., **102**, 517 (2010).
8. B.A. Howell, Y. Cui and D.B. Priddy, *J. Therm. Anal. Calorim*., **74**, 313 (2004).
9. M.Y. Keating and J.L. Howell, *J. Therm. Anal. Calorim*., **106**, 213 (2011).
10. M.Y. Keating, F. Gao and J.B. Ramsey, *J. Therm. Anal. Calorim*., **106**, 207 (2011).
11. Z.Q. Wang and S.M. Cohen, *J. Am. Chem. Soc*., **129**, 12368 (2007).
12. Y. Yoo, V. Varela-Guerrero and H.K. Jeong, *Langmuir*, **27**, 2652 (2011).
13. A.R. Millward and O.M. Yaghi, *J. Am. Chem. Soc*., **127**, 17998 (2005).
14. J. Gascon, U. Aktay, M.D. Hernandez-Alonso, G.P.M. van Klink and F. Kapteijn, *J. Catal*., **261**, 75 (2009).
15. L.C. Rowsel and O.M. Yaghi, *J. Am. Chem. Soc*., **128**, 1304 (2006).
16. B.D. Chandler and L.H. Pignolet, *Catal. Today*, **65**, 39 (2001).
17. V. Matsouka, M. Konsolakis, R.M. Lambert and I.V. Yentekakis, *Appl. Catal. B*, **84**, 715 (2008).
18. G. Hussain and M.M. Rahman, *Spectrochim. Acta A*, **64**, 880 (2006).
19. M. Eddaoudi, J. Kim, N. Rosi, D. Vodak, J. Wachter, M. O'Keeffe and O.M. Yaghi, *Science*, **295**, 469 (2002).
20. D. Kim, T.B. Lee, S.B. Choi, J.H. Yoon, J. Kim and S.H. Choi, *Chem. Phys. Lett*., **420**, 256 (2006).
21. L. Zhang and Y.H. Hu, *J. Phys. Chem. C*, **114**, 2566 (2010).
22. A.B. Fuertes and T.A. Centeno, *J. Mater. Chem*., **15**, 1079 (2005).
23. P.L. Feng, J.J. Perry, S. Nikodemski, B.W. Jacobs, S.T. Meek and M.D. Allendorf, *J. Am. Chem. Soc*., **132**, 15487 (2010).